A simple nonlinear analytical model for unconsolidated geotextile-encased sand columns

Hyeong-Joo Kim[1], *Voltaire Anthony Corsino Jr[2], Young-Soung Joung[3], Jun-Young Park[4], James Vincent Reyes[5]

[1] *Department of Civil Engineering, Kunsan National University, Gunsan 54150, South Korea*
[2], [3], [4], [5] *Department of Civil and Environmental Engineering, Kunsan National University, Gunsan 54150, South Korea*
[2] *vacorsino@kunsan.ac.kr*

ABSTRACT

In this study, a simple analytical model for unconsolidated geotextile-encased sand columns (GESACs) was presented. The model is based on the power law, and can take into account the effect of various soil and geotextile parameters including column diameter (D), varying geotextile stiffness (J), and soil friction angle (ϕ). A uniaxial compression test on GESAC was conducted in an effort to study the failure mechanism of the soil-geotextile system. To assess the proposed GESAC model, the uniaxial compression test was simulated. Based on the GESAC model, internal lateral stresses developed in the GESAC because of the confining effect of the geotextile, which resulted in the increase of tension force on the geotextile. It was shown that failure occurred as the tension force approached the seam strength of the geotextile. To verify the proposed model, data on GESACs in the uniaxial compression test found in the literature were analyzed, and it was shown that the proposed model was able to fairly predict the behavior of GESACs having various lengths and diameters.

1. INTRODUCTION

Geotextile wide applications have been an area of interest ever since early studies and reported cases of fabric materials being used in the same context as that of geotextile applications today (Lawson, 2008). Geotextiles have different types and different uses, some of which were described by Palmiera et al. (2008). Tubes or bags made out of geotextiles have been widely used for coastal and dewatering applications

---

[1] Professor
[2], [3], [4], [5] Graduate student

(Guo et al., 2015; Zhang et al., 2022). Tensile forces of these tubes in their fully filled state were studied by Leshchinsky et al. (1996), Plaut and Suherman (1998), Yee (2012), and others. Model tests, large-scale experiments, and numerical and analytical studies on the stability of geotextile tubes can be found in the works of Kriel (2012) and Kim et. al (2015) while consolidation modelling methods for tubes filled with fine grained materials were proposed by Brink et. al (2013) and Kim et al. (2021). Studies on the geotextile encasement of stone and sand columns have also been conducted in the literature (Chen et al., 2018; Khadim et al., 2018). Apart from their function as vertical drains, these stone and sand columns have been applied to improve the bearing capacity of soft ground (Basack et al., 2017; Salem et al., 2018). Due to the confining effect of the geotextile, the bearing capacity, stiffness, and seismic resistance of these columns are further improved (Dash and Bora, 2013; Cengiz and Güler, 2018).

However, there are only a few research focused on relating stresses, strain, relative density, geotextile properties, etc. to the shearing behavior of the soil-geotextile system. Fig. 1 shows a typical embankment design reinforced by geotextile tubes. As seen in this figure, the soil-geotextile system is exposed to different vertical and lateral loads per stacking level. Geotextile tensile loads induced by shearing, as well as the behavior of the entire system itself, require attention as there are many factors that affect its behavior. Khadim et al. (2018) have conducted three-dimensional numerical analysis on dense geotextile-encased sand columns (GESAC) based on the finite element method (FEM) using parameters calibrated from triaxial tests. In their study, an elastoplastic model was used to simulate the behavior of the GESAC. Khadim et al. (2018) stated that there were limitations to using the Mohr-Coulomb model, hence, the use of nonlinear methods could result in better representation of the behavior of GESACs. In addition, soil-geotextile interaction analysis of the results of their experiments were not conducted.
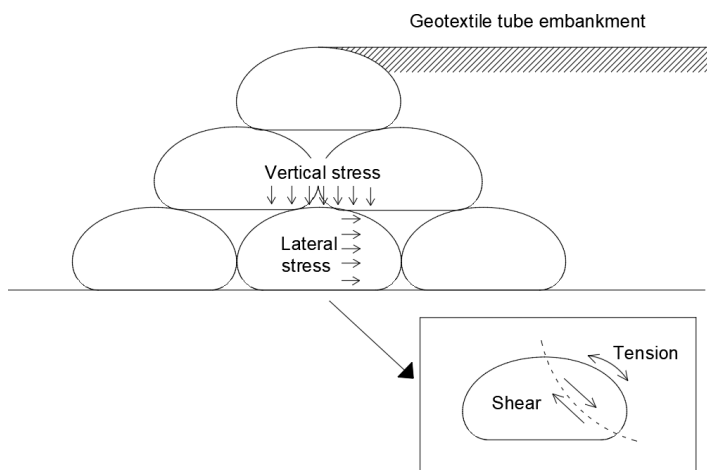

Fig. 1. Developed shear stresses during stacking

In an effort to further analyze the soil-geotextile interaction, a nonlinear analytical model for unconsolidated GESACs is proposed in this study. Determining the unconsolidated behavior of GESACs is important because this leads to the development

of an analytical model for consolidated GESACs. Xue et al. (2019) stated that the stress-strain behavior of consolidated geotextile-encased stone columns can be obtained by superposing the uniaxial compression curve of a geotextile-encased stone column to the compressive curve of the ordinary stone column in the triaxial test. This same concept can be applied to geotextile-encased sand columns, hence, determining the various factors that affect the unconsolidated behavior of GESACs is necessary for the advancement of the design of geotextile-encased soil systems. In this study, the behavior of GESACs is first investigated in the uniaxial compression test. Thereafter, the proposed model is verified based on data found in the literature on dense GESACs in the uniaxial compression test.

2. THEORETICAL BACKGROUND

The behavior of various geotextiles in a wide-width strip test (ASTM D4595) often vary from being elastic to nonlinearly concaving upward or downward, as shown in Fig. 1. The behavior can be represented using the power law, as shown in Eq. (1), wherein ε_g and T_g are the current strain and tension force of the geotextile, respectively, while $\varepsilon_{g,f}$ and $T_{g,f}$ are the strain and tension force at geotextile failure, respectively. In Eq. (1), n is a curve fitting parameter, which controls the curvature in which an $n < 1.0$ gives nonlinear curves concaving upward while $n > 1.0$ gives nonlinear curves concaving downward.
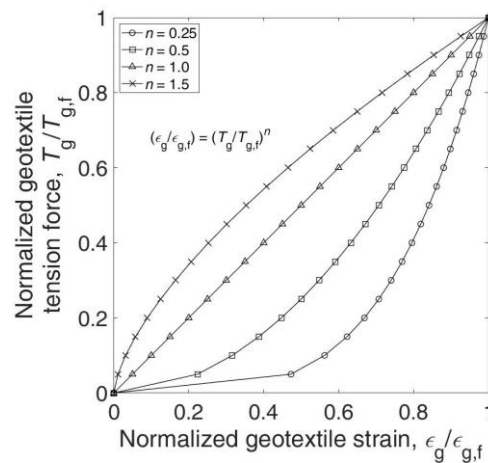

Fig. 1. Possible behavior of geotextiles in a wide-width strip test

$$\left(\frac{\varepsilon_g}{\varepsilon_{g,f}}\right) = \left(\frac{T_g}{T_{g,f}}\right)^n \tag{1}$$

The behavior of geotextile-encased sand columns (GESACs) in uniaxial compression tests and unconsolidated triaxial tests can be similarly represented by the power law using Eq. (2). In Eq. (2), $\Delta\sigma_v$ is the current change in vertical stress, ε_1 is the current axial strain, $\Delta\sigma_{v,f}$ is the change in vertical stress at geotextile failure, and $\varepsilon_{1,f}$ is

the axial strain at geotextile failure. In this study, $\Delta\sigma_{v,f}$ is related to $T_{g,f}$, the initial radius (r_0), $\varepsilon_{g,f}$, and the coefficient of active lateral pressure (K_a), as shown in Eq. (3), wherein the K_a can be approximated using the friction angle (ϕ) of the sand by Eq. (4). In addition, $\varepsilon_{1,f}$ is related to $\varepsilon_{g,f}$ and the Poisson's ratio of the GESAC at geotextile failure ($\upsilon_{sg,f}$), as shown in Eq. (5). Combining Eqs. (2), (3), and (5), ε_1 can be approximated using Eq. (6). In this study, the shear stress of the unconsolidated GESAC (q_{ucd}) is obtained by subtracting $\Delta\sigma_v$ with the change in radial stress ($\Delta\sigma_r$), as shown in Eq. (7). Combining Eqs. (6) and (7), the governing equation for q_{ucd} with respect to ε_1 is given by Eq. (8).

Based on ε_1, the current column height (H) can be obtained using Eq.(9) while the current radius (r) can be obtained based on $\Delta\sigma_r$ using Eq. (10). Given that $\Delta\sigma_r$ is known and that r is unknown in Eq. (10), r can only be determined numerically using an approximate solution. After which, only then can Eq. (1) be used to determine T_g based on ε_g determined from Eq. (10). The area of the column (A) can also be calculated using Eq. (11).

$$\varepsilon_1 = \left(\frac{\Delta\sigma_v}{\Delta\sigma_{v,f}}\right)^n \cdot \varepsilon_{1,f} \tag{2}$$

$$\Delta\sigma_{v,f} = \frac{T_{g,f}}{K_a \cdot r_0(1 + \varepsilon_{g,f})} \tag{3}$$

$$K_a = \frac{1 - \sin(\phi)}{1 + \sin(\phi)} \tag{4}$$

$$\varepsilon_{1f} = \frac{\varepsilon_{g,f}}{\upsilon_{sg,f}} \tag{5}$$

$$\varepsilon_1 = \left[\frac{\Delta\sigma_v \cdot K_a \cdot r_0(1 + \varepsilon_{g,f})}{T_{g,f}}\right]^n \cdot \frac{\varepsilon_{g,f}}{\upsilon_{sg,f}} \tag{6}$$

$$q_{ucd} = \Delta\sigma_v - \Delta\sigma_r = \Delta\sigma_v - \Delta\sigma_v \cdot K_a = \Delta\sigma_v(1 - K_a) \tag{7}$$

$$q_{ucd} = \left(\frac{\varepsilon_1 . \upsilon_{sg,f}}{\varepsilon_{g,f}}\right)^{1/n} \frac{T_{g,f}(1 - K_a)}{K_a \cdot r_0(1 + \varepsilon_{g,f})} \tag{8}$$

$$H = H_0(1 + \varepsilon_1) \tag{9}$$

$$r = r_0(1 + \varepsilon_g) = \frac{T_{g,f}}{\Delta\sigma_r}\left(\frac{\frac{r}{r_0} - 1}{\varepsilon_{g,f}}\right)^{1/n} \tag{10}$$

$$A = \pi r^2 = \pi \left[r_0 (1 + \varepsilon_g) \right]^2 \tag{11}$$

3. METHODS AND MATERIALS

The uniaxial compression test on geotextile-encased sand column (GESAC) was conducted in this study. The GESAC was prepared using a PVC pipe mold. A cylindrical geotextile column with an initial circumference of 64.5 cm and a height of about 40.5 cm was placed in the mold. Thereafter, Saemangeum silty sand having a water content of 18.54% was pluviated by air, and was compacted using a rammer. A sample with a relative density of about 65% was produced. The column was then installed to the universal testing machine, and was loaded until failure was observed. During testing, measurement of the radial strain (ε_3) or area (A) of the specimen was difficult. Hence, the compressive pressure ($\Delta\sigma_v$) during testing cannot be directly determined. To obtain A, the radial strain (ε_3), which is equivalent to geotextile strain (ε_g) during testing, were interpolated using the measured final radial strain ($\varepsilon_{3,f}$) and the applied vertical loads during testing. After obtaining ε_3 or ε_g, Eq. (11) was used to approximate A.

The Saemangeum silty sand was used, which was obtained from the Saemangeum river estuary near the airport of Gunsan city, South Korea. Several laboratory tests including sieve test, compaction test, and basic property tests were conducted, and the results are shown in Table 1. The soil contains a considerable amount of fines at about 22%, and its optimum moisture content is 15%. Polyester (PET) geotextile was used to encase the sand column. The geotextile was jointed using a flat seam with three-row stitches. The tensile properties were determined by conducting the wide-width strip test (ASTM-D4595). The load-strain relationship of the geotextile with joint in the wide-width strip test is shown in Fig. 2. The fitted curve using Eq. (1) is also shown in Fig. 2, and it can be seen that curve matches well with the measured data using an exponent n of 0.7.
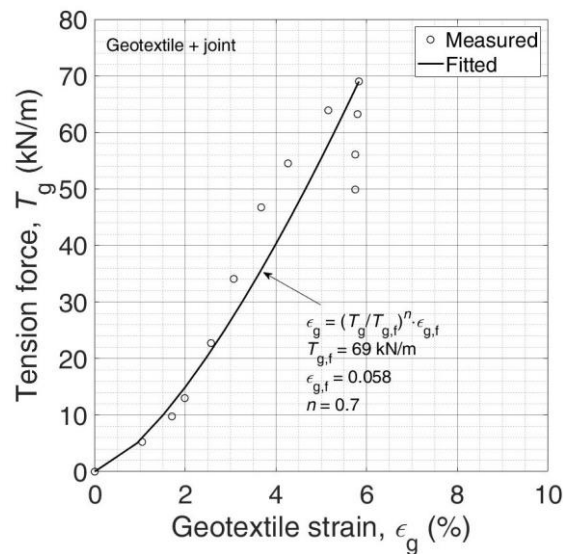

Figure with axes: Tension force, T_g (kN/m) vs Geotextile strain, ϵ_g (%). Legend: Measured (circles), Fitted (line). Text annotations: Geotextile + joint; $\epsilon_g = (T_g / T_{g,f})^n \cdot \epsilon_{g,f}$; $T_{g,f} = 69$ kN/m; $\epsilon_{g,f} = 0.058$; $n = 0.7$

Fig. 2. Result of wide-width strip test of PET geotextile used in this study

Table. 1. Properties of Saemangeum silty sand

Properties	Quantity
Specific gravity, G_s	2.69
Percentage passing #200 sieve (%)	22.20
Maximum dry unit weight, γ_{dmax} (kN/m³)	16.71
Minimum dry unit weight, γ_{dmin} (kN/m³)	11.43
Optimum moisture content (%)	15.0

4. RESULTS AND DISCUSSION

The result of the uniaxial compression test is shown in Fig. 3, and it can be seen that the sample failed at a compressive pressure of about 2250 kPa and at an axial strain ($\varepsilon_{1,f}$) of about 18%. The circumference of the sample was measured at the end of the test, and it was observed that the circumference increased by about an average of 6.2%. Hence, $u_{sg,f}$ was determined to be about 0.35. The failed sample was investigated visually, and it was ascertained that the cause of failure was at the seams, and that most of the circumferential elongation at the end of the test was experienced at the seams.

To assess the proposed GESAC model, the uniaxial compression test was simulated. For the GESAC model proposed in this study, K_a was determined as 0.27 using Eq. (4) based on a friction angle (ϕ) of 35°. The friction angle was determined from triaxial tests on Saemangeum silty sand having relative density of 65%. The exponent n was 0.7, the geotextile tension force at failure ($T_{g,f}$) was 69 kN/m, and the geotextile strain at failure ($\varepsilon_{g,f}$) was 0.058, as determined from Fig. 2. The Poisson's ratio of the GESAC at failure ($u_{sg,f}$) was 0.35, as determined after the uniaxial compression test.

A comparison between the measured and predicted axial strains with compressive pressure is also shown in Fig. 3. It can be seen that good agreement is observed between the measured data and the predicted data using the GESAC model. Due to the confining effect of the geotextile, lateral stresses developed during compressive loading, which is a similar reaction to that of retaining walls when vertical loads are applied. Due to the lateral stresses, the tension force in the geotextile increased, as shown in Fig. 4. It can be seen that the load at the end of the test ($\Delta\sigma_v$ = 2250 kPa) resulted in a hoop force of about 64 kN/m, which is close to the seam strength of the geotextile. After determining the vertical and lateral stresses, the relationship between the mean stress (p) and q was obtained, as shown in Fig. 5. It can be seen that the GESAC model follow the critical state line. Without geotextile encasement, the column would fail at very low compressive pressures. However, due to the confining effect of the geotextile, the p-q path continues to move along the critical state line, allowing the GESAC to carry larger compressive pressures.
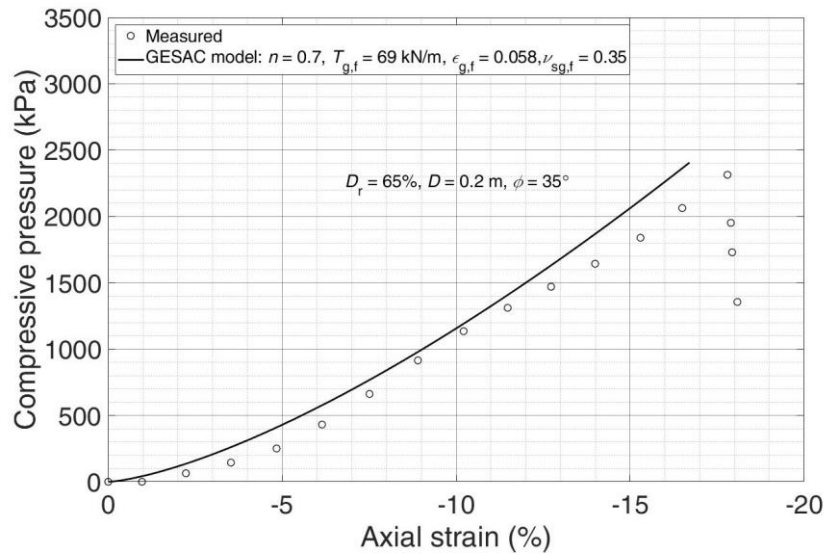
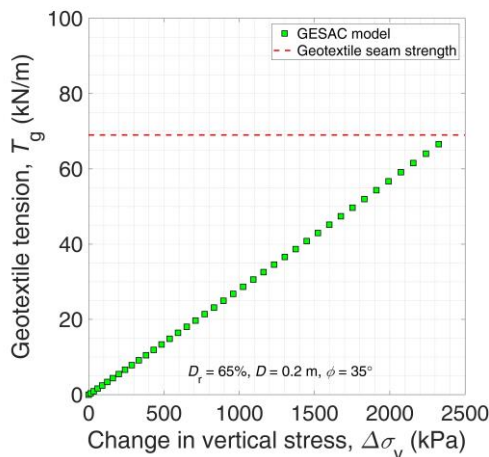Fig. 3. Result of uniaxial compression test on GESAC conducted in this study

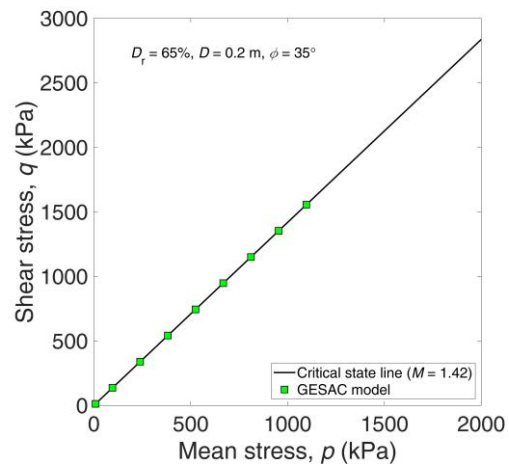Fig. 4. Predicted geotextile tension during uniaxial compression test

Fig. 4. Predicted *p-q* relationship during uniaxial compression test

5. VERIFICATION OF GESAC MODEL

Khadim (2016) investigated the vertical stability of geotextile-encased sand columns (GESACs) having diameters (D) of 15 cm in the uniaxial compression test. The Kansas river sand with relative density of about 70% was used in the experiment while woven geotextiles were used to encase the soil specimens. The friction angle of Kansas river at a relative density of about 70% was determined to be about 39° based on triaxial tests, and the strength of the woven geotextile in the cross-machine direction (CMD) and machine direction (MD) were determined to be 51 kN/m and 54 kN/m, respectively. A summary of the parameters for the geotextile used by Khadim (2016) is given in Table 2. In the predictions, the parameters of the machine direction were utilized, and the $u_{sg,f}$

was assumed to be 0.35, similar to what was obtained in section 4.

The results of the uniaxial compression tests are shown in Fig. 5. It can be seen that settlement increases with increase of column length. Using a friction angle (ϕ) of 39°, it can be seen that the GESAC model was able to predict the settlement of the columns at different length to diameter ratios. The prediction by the model shows different settlement results with L/D. However, the relationship between the change in vertical pressure ($\Delta\sigma_v$) and axial strain (ε_1) are actually the same, regardless of the length of the column. Based on the results, it can be hypothesized that the behavior of the unconsolidated GESACs in the uniaxial compression tests conducted by Khadim (2016) can be well-predicted using a $u_{sg,f}$ of 0.35.

Table 2. Parameters for geotextile used by Khadim (2016)

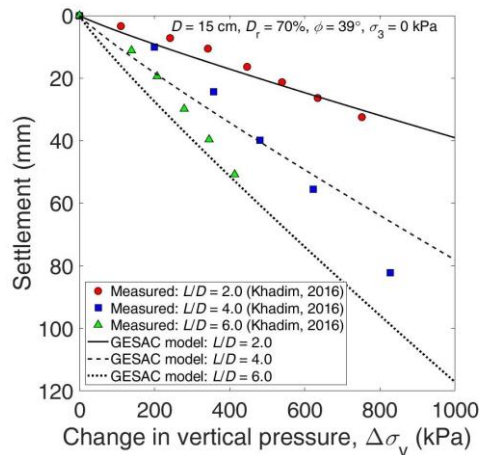| Property	Description
Material type	Elastic
Geotextile stiffness, J (kN/m)	418
Exponent n for machine direction	0.9
Tension force at failure, T_f (kN/m)	51

Fig. 5. Variation of settlement with $\Delta\sigma_v$ of GESAC in uniaxial compression test conducted by Khadim (2016)

6. CONCLUSIONS

In an effort to further analyze the soil-geotextile interaction of unconsolidated geotextile-encased sand columns (GESACs), an analytical model was proposed in this study. The behavior of GESAC was investigated in the uniaxial compression test to assess the GESAC model. Thereafter, the proposed model was verified based on data found in the literature on dense GESACs. Based on the results of this study, the following conclusions are drawn:

- The behavior of geotextiles in a wide-width strip test can be represented using a power law equation based on the strain at failure $\varepsilon_{g,f}$ and the tension force. The exponent n is a curve fitting parameter, which controls the curvature of the

curve.

- The behavior of GESACs in uniaxial compression tests or unconsolidated triaxial tests can be similarly represented by a power law equation using the same exponent *n* obtained from the wide-width strip tests.
- Based on GESAC model, internal lateral stresses develop in the GESAC because of the confining effect of the geotextile. Due to the internal lateral stresses, circumferential tension force on the geotextile increases while the *p-q* path of the GESAC follows the critical state line.
- It was shown in the uniaxial compression test on geotextile-encased Saemangeum silty sand that failure occurred as the tension force approached the seam strength of the geotextile.
- The settlement of GESAC increases with increase of length to diameter ratio. It was shown that the GESAC model can well-represent this phenomenon.
-

ACKNOWLEDGMENT

REFERENCES

Basack, S., Indraratna, B., Rujikiatkamjorn, C., Siahaan, F., 2017. Modeling the stone column behavior in soft ground with special emphasis on lateral deformation. J. Geotech. Geoenviron. Eng. 143 (6), p.04017016.

Brink, N.R., Kim, H.J., Znidarcic, D., 2013. Consolidation modelling for geotextile tubes filled with fine-grained material. In: Proceedings of the GhIGSGeoAfrica 2013 Conference, Accra, Ghana.

Chen, J.F., Wang, X.T., Xue, J.F., Zeng, Y., Feng, S.Z., 2018. Uniaxial compression behavior of geotextile encased stone columns. Geotext. Geomembranes, 46 (3), 277-283.

Cengiz, C., Güler, E., 2018. Seismic behavior of geosynthetic encased columns and ordinary stone columns. Geotext. Geomem. 46 (1), 40-51.

Dash, S.K., Bora, M.C., 2013. Influence of geosynthetic encasement on the performance of stone columns floating in soft clay. Can. Geotech. J. 50 (7), 754-765.

Guo, W., Chu, J., Zhou, B., 2015. Model tests on methods to improve dewatering efficiency for sludge-inflated geotextile tubes. Geosyn. Int. 22 (5), 380-392.

Kadhim, S.T., 2016. Stability analysis of geotextile encased sand columns, Ph.D. dissertation, University of Kansas, Kansan, USA.

Kadhim, S.T., Parsons, R.L., Han, J., 2018. Three-dimensional numerical analysis of individual geotextile-encased sand columns with surrounding loose sand. Geotext. Geomembranes, 46 (6), 836-847.

Kim, H.J., Dinoy, P.R., 2021. Two-dimensional consolidation analysis of geotextile tubes filled with fine-grained material. Geotext. Geomembranes, 49 (5), 1149-1164.

Kim, H.J., Won, M.S., Jamin, J.C., 2015. Finite-element analysis on the stability of geotextile tube–reinforced embankments under scouring. Int. J. Geomech. 15 (2), 06014019.

Kriel, H.J., 2012. Hydraulic stability of multi-layered sand-filled geotextile tube breakwaters under wave attack, MSc Thesis, Stellenbosch University, South Africa.

Lawson, C.R., 2008. Geotextile containment for hydraulic and environmental engineering. Geosyn. Int. 15 (6), 384-427.

Leshchinsky, D., Leshchinsky, O., Ling, H.I., Gilbert, P.A., 1996. Geosynthetic tubes for confining pressurized slurry: some design aspects. J. Geotech. Eng. 122 (8), 682-690.

Palmeira, E.M., Tatsuoka, F., Bathurst, R.J., Stevenson, P.E., Zornberg, J.G., 2008. Advances in geosynthetics materials and applications for soil reinforcement and environmental protection works. Elec. J. Geotech. Eng. 13, 1-38.

Plaut, R.H., Suherman, S., 1998. Two-dimensional analysis of geosynthetic tubes. Acta Mech., 129 (3-4), 207-218.

Salem, Z.B., Frikha, W., Bouassida, M., 2017. Effects of densification and stiffening on liquefaction risk of reinforced soil by stone columns. J. Geotech. Geoenviron. Eng., 143 (10), p.06017014.

Xue, J., Liu, Z. and Chen, J., 2019. Triaxial compressive behaviour of geotextile encased stone columns. *Computers and Geotechnics*, *108*, pp.53-60.

Yee, T.W., 2012. Analysis of geotextile tube using discrete membrane elements method. In: Proceedings of the Fifth European Geosynthetics Congress, Valencia, Spain, pp. 583-587.

Zhang, H., Wang, W.J., Liu, S.J., Chu, J., Sun, H.L., Geng, X.Y., Cai, Y.Q., 2022. Consolidation of sludge dewatered in geotextile tubes under combined fill and vacuum preloading. J. Geotech. Geoenviron. Eng. 148 (6), p.04022032.